Available online at www.sciencedirect.com
SCIENCE DIRECT
Biochimie ■■ (2006) ■■■
BIOCHIMIE
www.elsevier.com/locate/biochi

Energy landscape of the ribosomal decoding center

K.Y. Sanbonmatsu

Theoretical Biology and Biophysics Department, Los Alamos National Laboratory, MS K710, 87545 Los Alamos, NM, USA

Received 9 February 2006; accepted 27 June 2006

Abstract

The ribosome decodes the genetic information that resides in nucleic acids. A key component of the decoding mechanism is a conformational switch in the decoding center of the small ribosomal subunit discovered in high-resolution X-ray crystallography studies. It is known that small subunit nucleotides A1492 and A1493 flip out of helix 44 upon transfer RNA (tRNA) binding; however, the operation principles of this switch remain unknown. Replica molecular dynamics simulations reveal a low free energy barrier between flipped-out and flipped-in states, consistent with a switch that can be controlled by shifting the equilibrium between states. The barrier determined by the simulations is sufficiently small for the binding of ligands, such as tRNAs or aminoglycoside antibiotics, to shift the equilibrium.

Keywords: Ribosome; Decoding center; Simulation; Replica; REMD; RNA; tRNA selection; Base flip

1. Introduction

The ribosome implements the genetic code by translating information residing in nucleic acid into protein, a process central to biological systems. During translation, the ribosome must decode genetic information, based on a four nucleotide alphabet, into a protein sequence, based on a twenty amino acid alphabet [1–3]. To accomplish this feat, it uses a molecular look-up table, embodied by the set of transfer RNAs (tRNAs), which convert three-letter codons into one-letter amino acids, according to the genetic code. During each round of decoding, the ribosome searches through the table for a correct match with the messenger RNA (mRNA) codon by binding tRNAs (in the form of aminoacyl–tRNA:EF–Tu:GTP ternary complexes), incorporating only the matching amino acid into the nascent polypeptide chain [4]. Because the ribosome is the only molecular machine able to transform one long string of information into another long string of information using a non-trivial look-up table operation, it is analogous to the central processing unit (CPU) of a computer.

The mechanism by which the ribosome is able to decode genetic information has been studied for 40 years and is still unsolved at the molecular level [5]. A key conformational change that occurs during decoding is the flipping of two universally conserved 16S rRNA adenines (A1492 and A1493). Early NMR studies suggested that these two adenines are disordered and may have several different flipped-in substates [6]. The Ramakrishnan group has shown that bases A1492 and A1493, which normally reside inside a helix (small subunit helix SH44), flip out of the helix upon tRNA binding, interacting simultaneously with the tRNA anticodon and the mRNA codon [7]. This transition is accompanied by a flip of G530 from the syn to antisyn configuration. Here, the term 'flipping' refers to a shift in equilibrium between the flipped-in and flipped-out states. Furthermore, there is likely to be a distribution both of flipped-in conformations and flipped-out conformations, each characterized by a basin of finite extent in configuration-space. The process of flipping and the associated change in free energy correspond to the transition between basins.

The X-ray structure shows the flipped-in state to have high B-factors, suggesting that A1492 and A1493 are somewhat disordered in the flipped-in state. The flipped-out state has relatively low B-factors, suggesting that the tRNA significantly stabilizes the flipped-out state [7]. When in the flipped-out state, A1492–A1493 form five hydrogen bonds with the codon–anticodon minihelix, demonstrating their key role in decoding. The importance of these hydrogen bonds has been

E-mail address: kys@lanl.gov (K.Y. Sanbonmatsu).

0300-9084/$ - see front matter © 2006 Published by Elsevier SAS.
doi:10.1016/j.biochi.2006.06.012

underscored by recent biochemical experiments demonstrating the significant effect on A-site tRNA binding produced by the removal of these hydrogen bonds [8,9]. A1492, A1493 and G530 are not only universally conserved, but have lethal mutant phenotypes [10–12].

A1492 and A1493 are positioned in an unstable configuration in the decoding center helix and are prone to flip out of the helix (Fig. 1). In particular, A1492 and A1493 are shared by A1408 in a 2:1 bulge with A:A non-Watson–Crick base pair geometries [7,13,14]. The helix itself is not A-form, but is curved at the point of this bulge. The decoding helix is effectively designed to facilitate the flipping of A1492–A1493 and may act as a switch convert the ribosome from rejecting to accepting states during decoding.

Numerous structural studies have been performed on the decoding center helix (small subunit helix 44) in complex with antibiotics [15]. NMR studies have determined the solution structure of the decoding center helix in the presence of the aminoglycosides gentamicin and paromomycin for prokaryotic and eukaryotic wild type systems, as well as various resistant mutants [16–23]. High-resolution X-ray structures of the decoding center helix have determined the precise hydrogen bond network between the antibiotic and the decoding center for a large suite of antibiotics, including paromomycin, tobramycin and geneticin [24–26]. Similar structures have been solved for several resistant mutants [27] and, most recently, for the case of *H. sapiens* [28]. The *H. sapiens* structure demonstrates that the decoding helix may have multiple flipped-in conformations. The decoding bases were found to flip upon binding of aminoglycosides for the isolated decoding center helix and for the intact small ribosomal subunit [13,29].

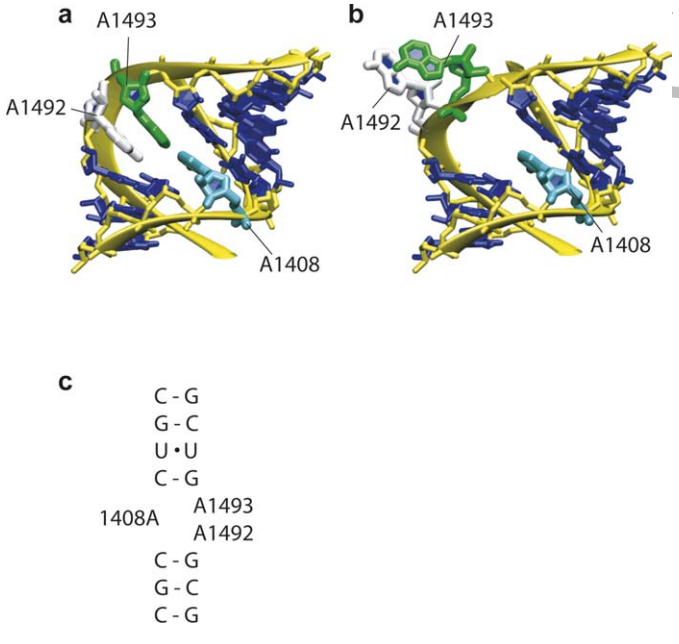

Fig. 1. The ribosomal decoding center helix. X-ray structure of the 16S rRNA SH44 decoding center helix in the (a) flipped-in and (b) flipped-out configurations, used as initial structures in the REMD simulations. Cyan, A1408; white, A1492; green, A1493; yellow, backbone; blue, bases. (c) Secondary structure of decoding center helix shows the unstable 2:1 bulge with A:A non-Watson–Crick pairs. A1408 is shared by A1492 and A1493.

While X-ray structures of the small subunit in the presence of cognate tRNA anticodon stem loops (ASLs) show both A1492 and A1493 flipped-out, structures in the presence of near-cognate ASLs in absence of antibiotics show A1493 flipped-out and A1492 flipped-in [30]. Recent structures of the 70S ribosome show A1493 and A1492 flipped-out in one conformation, and A1493 alone flipped-out in a second conformation [31].

In reality, an equilibrium between the flipped-in and flipped-out configurations exists, which is shifted towards the flipped-in configuration in absence of cognate tRNAs, and towards the flipped-out configuration in the presence of cognate tRNAs. Near-cognate tRNAs represent an intermediate case, where non-Watson–Crick codon–anticodon base pairs alter the geometry of the codon–anticodon minihelix. In this case, the codon–anticodon–ribosome hydrogen bonds may be weakened sufficiently to shift the equilibrium from flipped-out to flipped-in. The shift in equilibrium depends on the difference in free energy between the flipped-in and flipped-out states, as well as the size of the activation barrier.

Fast flipping will allow slight differences between cognate and near-cognate anticodons to change the flipping equilibrium. Slow flipping, or a high flipping barrier, will require a large change to trigger base-flipping, such as the binding of a tRNA molecule. In this case, we would expect the decoding bases to be in the flipped-out configuration for both cognate and near-cognate tRNAs. Finally, a low flipping barrier may allow the decoding bases to flip in and out during translocation in order to grip and release the mRNA molecule [8]. Here, we explore the energy landscape of the decoding center to estimate the change in free energy and the activation barrier height of decoding base flip events.

With regard to computational methods, replica simulations (replica exchange molecular dynamics or REMD) have previously helped elucidate the thermodynamics of protein folding systems [32–35]. With respect to the ribosome, Harvey and coworkers created a structural model of the tRNA–rRNA–mRNA interaction [36,37]. Several dynamics modeling studies have been performed [38–44]; however, to date, no thermodynamics simulations of the ribosome have been performed.

Here, the replica method used in protein folding simulations is applied to the conformational switch in the decoding center. We emphasize that protein folding differs significantly from base-flipping events. In base-flipping, the total root mean squared deviation (RMSD) during the conformational change of the decoding region of SH44 is 2.97 Å, much smaller than the RMSD change that occurs during the folding of a small peptide. The base-flipping RMSD is comparable to the width of a single free energy basin in a protein folding simulation, rather than the distance traveled during a transition between basins [34,45]. While base-flipping barriers are relatively high in the case of Watson–Crick base pairs in DNA helices, we expect the barrier to be significantly lower in the case of the decoding helix because of the unusual geometry and non-

Watson–Crick nature of the flipping bases. Thus, we expect base-flipping simulations of the decoding center to require less sampling than protein folding and DNA systems. REMD enhances conformational sampling by a factor of ~35 over traditional single-temperature molecular dynamics simulation techniques [32,46].

2. Methods

The replica algorithm is characterized by performing simulations of a large number of copies of the original system to obtain a temperature distribution of the configurations available to a particular biomolecular system [47]. Copies of the system, identical except for temperature, exchange temperatures after a given time interval, avoiding kinetic traps by sampling high temperatures. This temperature sampling facilitates barrier crossings on the energy landscape (i.e. transitions between stable configurations), which may be prohibited by large barriers occurring at low temperatures. Precisely, a distribution of target temperatures T_1, ... T_i, T_j, ..., T_M is chosen for M replicas, whose coordinates are represented by q_1, ..., q_m, q_n, ..., q_M. Each replica attempts to exchange temperatures with another replica system using the Monte Carlo criterion:

$$P(\text{exchange}) = \exp(1/kT_i - 1/kT_j)\left(E_{(qm)} - E_{(qn)}\right)$$

Because the number of time steps between exchange attempts is much greater than unity, the communication requirements of this method are minimal, resulting in near-linear scaling of simulation speed-up with processor number.

The initial structures consisted of 16S rRNA nucleotides 1404–1411 and 1489–1497 from the small subunit structures of Ramakrishnan (PDB accession code 1J5E and 1IBM) [7,14]. The starting structures consisted of four configurations: (1) both A1492–A1493 flipped-in (1J5E); (2) both A1492–A1493 flipped-out (1IBM); (3) A1492 flipped-in and A1493 flipped-out; and (4) A1492 flipped-out and A1493 flipped-in. Configurations (3) and (4) were modeled by superposing (1) and (2). Excess ions were placed randomly in a box of $(55\ \text{Å})^3$ at concentrations of 0.1 M KCl and 7 mM $MgCl_2$. The molecular dynamics protocol was inspired by the extensive set of RNA simulations of Auffinger and Westhof [48–52]. The system was solvated with TIP3P water (N_{atoms} = 16,389), minimized, and subsequently equilibrated at constant temperature (T = 300 K) for 50 ps using a time step of 2 fs and the AMBER force field with particle mesh Ewald electrostatics [53]. To mimic the context of the small ribosomal subunit, the ends of SH44 (C1404, C1411, G1489 and G1497) were restrained by a harmonic potential of 1 kcal/mol Å^2. We used a method described previously in [32] to obtain a temperature distribution of 48 replicas in the range of $312.0 < T < 544.5$ K. The system was run in production exchange mode for 5.62 ns per replica, with exchange attempts every 0.25 ps, giving a total sampling of ~ 0.27 μs.

The choice of order parameter is crucial to the interpretation of the simulation results. Torsional parameters do not uniquely describe the flipping-in and flipping-out of 16S rRNA bases A1492–A1493. Rotational helical parameters (tip, inclination, opening, propeller, buckle, twist, roll, and tilt) also fail to uniquely capture base-flipping, in the sense that other conformations besides flipped-in and flipped-out conformations display values similar to those of the flipped-in and flipped-out conformations. Base pair hydrogen bond distances are also incapable of uniquely describing the flipping in/out. We use the order parameter, θ, defined by MacKerell, which defines a pseudo-dihedral angle between the center of mass of the neighboring base pair (C1407:G1491), the neighboring sugar (G1491), the sugar (A1492) and the base (A1492) of flipping nucleotides [54,55]. A similar definition was used for A1493.

The free energy landscape of the decoding base-flip conformational change is obtained using the potential-of-mean-force (PMF), $w = -kT \ln P(\mathbf{r})$, where $P(\mathbf{r}) = n_\mathbf{r}/N$ is the probability of the system residing in state $\mathbf{r}$, $n_\mathbf{r}$ is the number of configurations of state $\mathbf{r}$ sampled during the simulation, N is the total number of configurations sampled, $\mathbf{r}$ is a $3N_0$-dimensional state vector describing the configuration, and N_0 is the number of solute atoms. The PMF is equal to the change in free energy required to move the system from any of the sampled states to the specific state, $\mathbf{r}$. The change in free energy due to base-flipping is estimated by subtracting the flipped-in value of the PMF (i.e. the value of the minimum of the flipped-in basin) from the flipped-out value of the PMF. Figures were generated using VMD [56].

3. Results

The free energy landscape as determined by the potential-of-mean force surface on the (θ, T)-plane displays the conformational space sampled by A1492 and A1493 during the simulation (Fig. 2). The landscapes of A1492 and A1493 both show a major basin corresponding to the flipped-in state and several smaller flipped-out basins. The surface is rugged in both the θ-direction and the T-direction. Although the relative barrier heights show a tendency to decrease as a function of temperature, the landscape is far from monotonic as a function of temperature for a given value of θ. The advantage of the replica method is shown explicitly by the A1493 landscape (Fig. 2), where θ-values, which are forbidden at low temperatures (e.g. $\theta \sim -100°$), are easily accessible at higher temperatures.

The sampled configurations define the flipped-in and flipped-out basins in the free energy landscape. That is, the flipped-in basin consists of pseudo-dihedral angles in the range, $-5° < \theta < 60°$. Configurations outside of this range are considered to be flipped-out. Typical configurations for the flipped-in and flipped-out states are shown in Fig. 2. More examples of conformations corresponding to various values of θ are shown in Fig. 3 for the case of A1492.

A base-flipping event is defined as a conformational change of either A1492 or A1493 into or out of its respective flipped-in basin. Many base-flipping transitions were observed for A1492 and A1493, including single-base transitions and transitions in which A1492 and A1493 flip in or out of SH44 simul-

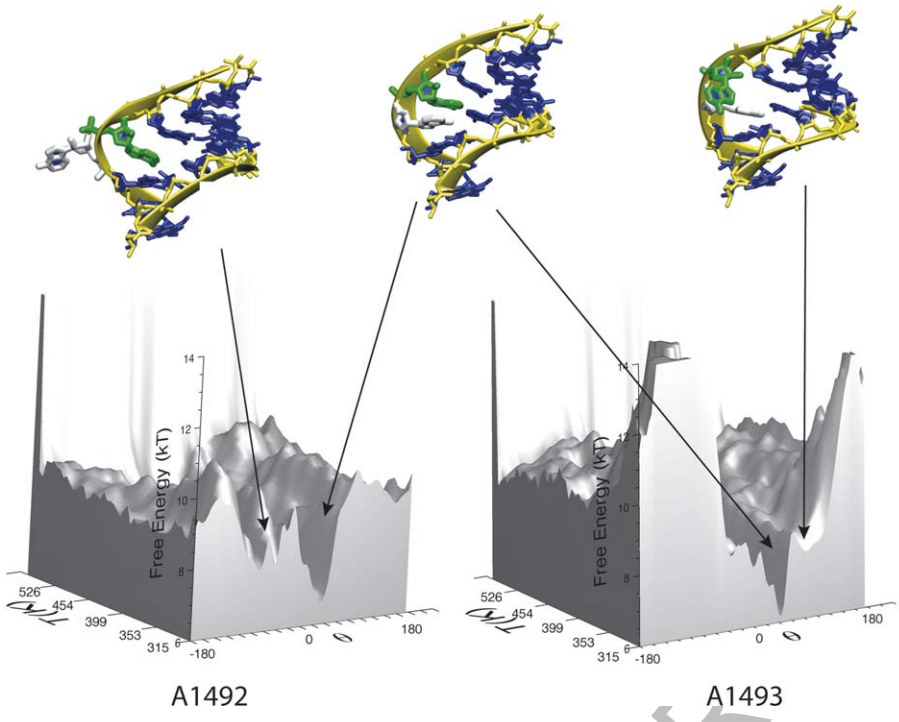

Fig. 2. Energy landscape of the ribosomal decoding center helix. Lower left: Free energy as a function of (θ, T) for A1492, where θ is the flipping pseudo-dihedral angle defined in the text. Lower right: Free energy as a function of (θ, T) for A1493. Structures depict typical configurations for the flipped-out (left and right) and flipped-in (middle) basins. White, A1492; green, A1493.

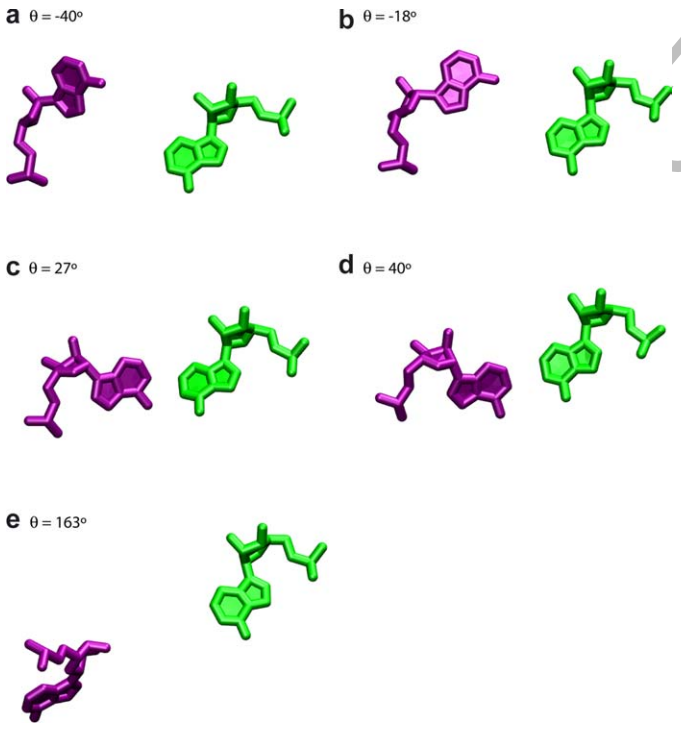

Fig. 3. Examples of conformations of 16S rRNA nucleotides A1492 (magenta) and A1408 (green) for different values of θ. The flipped-in basin includes $-5° < \theta < 60°$. The flipped-out state of A1492 is defined by all other values of θ. (a–b) Partially flipped-out state. (c–d) Flipped-in state. (e) Fully flipped-out state.

taneously. An example of a tandem-flipping events is shown in Fig. 4, where A1492 and A1493 simultaneously change configurations from the flipped-out state to the flipped-in state. Quantitatively, A1492 is said to undergo a flipping-out event when its trajectory passes from ($-5 < \theta < 60°$) to ($\theta < -80°$ or $\theta > 135°$). A1493 is said to undergo a flipping-out event when its trajectory passes from ($0 < \theta < 50°$) to ($\theta < -75°$ or $\theta > 125°$). The event definition uses a 75° barrier crossing buffer to eliminate spurious fluctuations near the barrier, ensuring bonafied crossing events. Because the size of the flipped-in basin differs for A1492 and A1493 (Fig. 2), the quantitative definition of a flipping event also differs for A1492 and A1493. While some of the base-flipping events occur rapidly ($\tau_{flip} \sim 10$ ps), many flipping events occur quite gradually, with the base adopting several metastable intermediate conformations. In these cases the transition occurs over several hundred picoseconds, with some trajectories displaying events occurring over the course of a nanosecond. In all, 211 flipping events were observed for A1492 and 1089 events for A1493, yielding approximately fivefold times more flipping events for A1493 in comparison to A1492. On average, approximately 27 flipping events (of either A1492 or A1493) were observed per replica. We emphasize that these events result from the stochastic heating and cooling of each replica. While replica simulations produce the thermodynamics of the system, they do not capture kinetics. The flipping timescale may be estimated from replica simulations using the autocorrelation time of the order

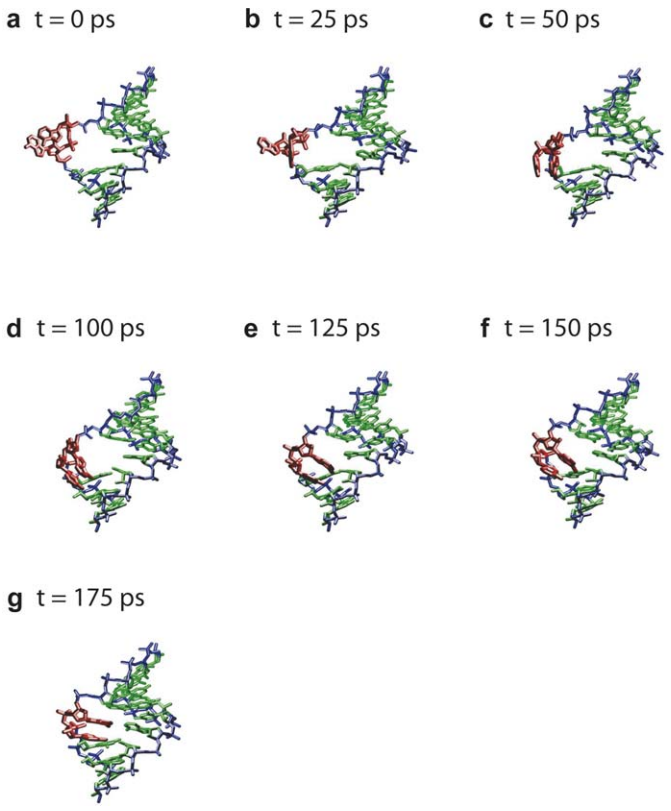

Fig. 4. Tandem flipping events. Several flipping events were observed where both A1492 and A1493 flipped-in or out of SH44 simultaneously. Time series of one such event is shown. Time is measured from the beginning of the transition event. Red, A1492 and A1493; blue, backbone; green bases.

parameter and a quasiharmonic approximation for the flipped-in free energy basin [34]. While this is beyond the scope of this short letter, these estimates are currently being computed. It should be noted that the number of flipping events is sensitive to the choice of order parameter and may be lower for an improved choice of order parameter.

Consistent with the X-ray crystallography structures, the simulations show the flipped-in states to be more energetically favorable than the flipped-out states. States with A1492 or A1493 completely flipped-out ($\theta \sim 180°$) are rarely sampled, while states with the adenines partially flipped-out are sampled more often. The energy landscape shows a change in free energy between flipped-in and flipped-out of 0.66 and 1.01 kcal/mol for A1492 and A1493, respectively. The barrier heights of these flipping transitions are 1.68 and 1.38 kcal/mol for A1492 and A1493, respectively. The results may differ when more extensive sampling is obtained, considering that these simulations only had ~ 0.27 μs sampling. Furthermore, the free energy values may also depend on the force field parameters and the order parameter.

4. Discussion

The simulations suggest that a dynamic equilibrium exists between the flipped-in and flipped-out states of A1492 and A1493. While conformational sampling is an important factor in obtaining realistic simulations of RNA systems, even an infinite amount of sampling will not produce accurate results without a corresponding accurate force field. A tremendous amount of outstanding work has produced the high quality force fields available today. Despite differences in force field parameterization techniques, recent versions of AMBER [57], CHARMM [58,59] and BMS [60] each produce reasonable properties of DNA for explicit solvent simulations [61]. Molecular dynamics simulations of nucleic acids using these force fields show good agreement with X-ray and NMR data with regards to torsional and helical parameters [48,51,61–64]. Despite these successes, there is still room for improvement. The groove widths appear to differ depending on the force field used [61]. Additionally, these three force fields are additive in their treatment of electrostatic interactions, using partial charges to approximate the effect of polarization [61,65]. While this approximation results in reasonably accurate hydrogen bonds (including angular dependence) [61], the polarization effect is included in an ad-hoc manner and is not included explicitly. While most simulations using explicit treatment of polarization have been performed on solvent alone, several recent simulations of proteins have been performed [61]. The partially covalent nature of hydrogen bonds is also neglected in additive force fields [66]. Enhanced sampling simulations represent one method of revealing previously unnoticed deficiencies in the force field that have not been tested with sufficiently long time scale sampling [67]. Ideally, an iterative process of realistic time scale simulation, thermodynamics experiments, comparison with experiment, and adjustment of force field parameters will produce closer convergence between theory and experiment.

The purpose of this short letter is to illuminate, qualitatively, the issues involved with respect to decoding and the thermodynamics of decoding base-flip transitions. Our estimate of $\Delta G_{\text{flip}} \sim 0.8$ kcal/mol (averaged over A1492 and A1493) suggests that the flipping is fast and may allow slight differences between cognate and near-cognate anticodons to change the flipping equilibrium. The simulations are consistent with a slightly favorable flipped-in state in absence of ligands. We emphasize that due to limitations in sampling and force field accuracy, it is difficult to assign error bars to our estimate. The accuracy of the simulation can be tested with corresponding fluorescence and thermodynamics studies of decoding helix base-flipping. In particular, fluorescence studies of the A-site helix with 2-aminopurine substitutions of A1492 and A1493 have displayed flipped-in or flipped-out states [68]. If these studies are correlated to thermodynamics studies of the same systems, it may possible to estimate values of ΔG, validating our simulations. Given the uncertainties of the simulations, we would consider experimental values of 0.5–5 kcal/mol for flipping validation of our simulation.

If the decoding nucleotides are continuously flipping in and out of SH44, ligands (aminoacyl-tRNAs and aminoglycoside antibiotics) might activate the decoding switch by trapping the bases in the flipped-out state. In particular, the presence of a cognate tRNA would be sufficient to shift the equilibrium

from the flipped-in state to the flipped-out state. In cases of near-cognate tRNAs bound to the ribosome lacking a single rRNA–tRNA hydrogen bond relative to the cognate tRNA in the flipped-out state, the change in the decoding center energy landscape due to the presence of the tRNA may not be large enough to shift the equilibrium completely to the flipped-out state. The shift in equilibrium to the flipped-in state for both A1492 and A1493 will result in the loss of four hydrogen bonds and the likely rejection of the tRNA.

The tandem flipping events observed in the simulation suggest that the stacking energy is significant. In the flipped-in state of the both the simulations and the X-ray structure, the bases are not entirely flipped-in. Thus, the strongest stacking interactions that A1492 and A1493 encounter may be with each other. Simulations of the decoding helix in the presence of cognate and near-cognate tRNAs will demonstrate whether or not A1492 and A1493 are indeed the decoding switch.

Acknowledgements

The author is grateful to Andrea Vaiana for useful discussions concerning the analysis and interpretation of the simulation data. The work was supported by the LANL LDRD program and NIH grant R01-GM072686.

References

[1] J.D. Watson, Involvement of RNA in the synthesis of proteins, Science 140 (1963) 17–26.
[2] W. Gilbert, Polypeptide synthesis in *Escherichia coli*, J. Mol. Biol. 6 (1963) 389–403.
[3] J. Davies, W. Gilbert, L. Gorini, Streptomycin, suppression and the code, Biochemistry 51 (1964) 883–890.
[4] J.M. Ogle, V. Ramakrishnan, Structural insights into translational fidelity, Annu. Rev. Biochem. 74 (2005) 129–177.
[5] M.V. Rodnina, W. Wintermeyer, Fidelity of aminoacyl-tRNA selection on the ribosome: kinetic and structural mechanisms, Annu. Rev. Biochem. 70 (2001) 415–435.
[6] J.D. Puglisi, et al., Aminoglycoside Antibiotics and Decoding, ASM Press, 2000.
[7] J.M. Ogle, D.E. Brodersen, W.M. Clemons Jr., M.J. Tarry, A.P. Carter, V. Ramakrishnan, Recognition of cognate transfer RNA by the 30S ribosomal subunit, Science 292 (2001) 897–902.
[8] S.S. Phelps, O. Jerinic, S. Joseph, Universally conserved interactions between the ribosome and the anticodon stem-loop of A site tRNA important for translocation, Mol. Cell 10 (2002) 799–807.
[9] R.P. Fahlman, M. Olejniczak, O.C. Uhlenbeck, Quantitative analysis of deoxynucleotide substitutions in the codon–anticodon helix, J. Mol. Biol. 355 (2006) 887–892.
[10] T. Powers, H.F. Noller, Dominant lethal mutations in a conserved loop in 16S ribosomal-RNA, Proc. Natl. Acad. Sci. USA 87 (1990) 1042–1046.
[11] J.J. Cannone, S. Subramanian, M.N. Schnare, J.R. Collett, L.M. D'Souza, Y. Du, B. Feng, N. Lin, L.V. Madabusi, K.M. Muller, N. Pande, Z. Shang, N. Yu, R.R. Gutell, The comparative RNA web (CRW) site: an online database of comparative sequence and structure information for ribosomal, intron, and other RNAs, BMC Bioinformatics 3 (2002) 2.
[12] S. Yoshizawa, et al., Recognition of the codon–anticodon helix by ribosomal RNA, Science 285 (1999) 1722–1725.
[13] A.P. Carter, W.M. Clemons, D.E. Brodersen, R.J. Morgan-Warren, B.T. Wimberly, V. Ramakrishnan, Functional insights from the structure of the 30S ribosomal subunit and its interactions with antibiotics, Nature 407 (2000) 340–348.
[14] B.T. Wimberly, D.E. Brodersen, W.M. Clemons Jr., R.J. Morgan-Warren , A.P. Carter, C. Vonrhein, T. Hartsch, V. Ramakrishnan, Structure of the 30S ribosomal subunit, Nature 407 (2000) 327–339.
[15] T. Hermann, Drugs targeting the ribosome, Curr. Opin. Struct. Biol. 15 (2005) 355–366.
[16] D. Fourmy, et al., Structure of the A site of *Escherichia coli* 16S ribosomal RNA complexed with an aminoglycoside antibiotic, Science 274 (1996) 1367–1371.
[17] D. Fourmy, et al., Paromomycin binding induces a local conformational change in the A-site of 16 S rRNA, J. Mol. Biol. 277 (1998) 333–345.
[18] S. Yoshizawa, et al., Structural origins of gentamicin antibiotic action, EMBO J. 17 (1998) 6437–6448.
[19] M.I. Recht, et al., Effect of mutations in the A site of 16S rRNA on aminoglycoside antibiotic–ribosome interaction, J. Mol. Biol. 286 (1999) 33–43.
[20] M.I. Recht, et al., Basis for prokaryotic specificity of action of aminoglycoside antibiotics, EMBO J. 18 (1999) 3133–3138.
[21] S.R. Lynch, J.D. Puglisi, Structure of a eukaryotic decoding region A-site RNA, J. Mol. Biol. 306 (2001) 1023–1035.
[22] S.R. Lynch, J.D. Puglisi, Structural origins of aminoglycoside specificity for prokaryotic ribosomes, J. Mol. Biol. 306 (2001) 1037–1058.
[23] S.R. Lynch, et al., Comparison of X-ray crystal structure of the 30S subunit-antibiotic complex with NMR structure of decoding site oligonucleotide–paromomycin complex, Structure (Camb) 11 (2003) 43–53.
[24] Q. Vicens, E. Westhof, Crystal structure of paromomycin docked into the eubacterial ribosomal decoding A site, Structure 9 (2001) 647–658.
[25] Q. Vicens, E. Westhof, Crystal structure of a complex between the aminoglycoside tobramycin and an oligonucleotide containing the ribosomal decoding a site, Chem. Biol. 9 (2002) 747–755.
[26] Q. Vicens, E. Westhof, Crystal structure of geneticin bound to a bacterial 16S ribosomal RNA A site oligonucleotide, J. Mol. Biol. 326 (2003) 1175–1188.
[27] P. Pfister, et al., The molecular basis for A-site mutations conferring aminoglycoside resistance: relationship between ribosomal susceptibility and X-ray crystal structures, ChemBioChem 4 (2003) 1078–1088.
[28] J. Kondo, et al., Two conformational states in the crystal structure of the *Homo sapiens* cytoplasmic ribosomal decoding A site, Nucleic Acids Res. 34 (2006) 676–685.
[29] Q. Vicens, E. Westhof, Crystal structure of paromomycin docked into the eubacterial ribosomal decoding A site, Structure 9 (2001) 647–658.
[30] J.M. Ogle, et al., Selection of tRNA by the ribosome requires a transition from an open to a closed form, Cell 111 (2002) 721–732.
[31] B.S. Schuwirth, et al., Structures of the bacterial ribosome at 3.5 Å resolution, Science 310 (2005) 827–834.
[32] K. Sanbonmatsu, A. Garcia, Structure of Met-enkephalin in explicit aqueous solution using replica exchange molecular dynamics, Proteins Struct. Function Genetics 46 (2002) 225–234.
[33] A. Garcia, K. Sanbonmatsu, Alpha-helical stabilization by side chain shielding of backbone hydrogen bonds, Proc. Natl. Acad. Sci. USA 99 (2002) 2782–2787.
[34] A. Garcia, K. Sanbonmatsu, Exploring the energy landscape of a beta hairpin in explicit solvent, Proteins Struct. Function Genetics 42 (2001) 345–354.
[35] S. Gnanakaran, et al., Peptide folding simulations, Curr. Opin. Struct. Biol. 13 (2003) 168–174.
[36] M.S. VanLoock, et al., Major groove binding of the tRNA/mRNA complex to the 16 S ribosomal RNA decoding site, J. Mol. Biol. 285 (1999) 2069–2078.
[37] M. VanLoock, et al., Movement of the decoding region of the 16 S ribosomal RNA accompanies tRNA translocation, J. Mol. Biol. 304 (2000) 507–515.
[38] K.Y. Sanbonmatsu, S. Joseph, Understanding discrimination by the ribosome: stability testing and groove measurement of codon–anticodon pairs, J. Mol. Biol. 328 (2003) 33–47.
[39] K.Y. Sanbonmatsu, et al., Simulating movement of tRNA into the ribosome during decoding, Proc. Natl. Acad. Sci. USA 102 (2005) 15854–15859.
[40] N. Spackova, J. Sponer, Molecular dynamics simulations of sarcin-ricin rRNA motif, Nucleic Acids Res. 34 (2006) 697–708.

[41] M. Kim, et al., A comparison between elastic network interpolation and MD simulation of 16S ribosomal RNA, J. Biomol. Struct. Dyn. 21 (2003) 395–405.
[42] J. Trylska, V. Tozzini, J.A. McCammon, Exploring global motions and correlations in the ribosome, Biophys. J. 89 (3) (2005) 1455–1463.
[43] F. Tama, et al., Dynamic reorganization of the functionally active ribosome explored by normal mode analysis and cryo-electron microscopy, Proc. Natl. Acad. Sci. USA 100 (2003) 9319–9323.
[44] W. Li, et al., Binding interactions between the core central domain of 16S rRNA and the ribosomal protein S15 determined by molecular dynamics simulations, Nucleic Acids Res. 31 (2003) 629–638.
[45] A. Garcia, J. Onuchic, Folding a protein in a computer: an atomic description of the folding/unfolding of protein A, Proc. Natl. Acad. Sci. USA 100 (2003) 13898–13903.
[46] W. Zhang, et al., Convergence of replica exchange molecular dynamics, J. Chem. Phys. 123 (2005) 154105.
[47] Y. Sugita, Y. Okamoto, Replica-exchange molecular dynamics method for protein folding, Chem. Phys. Lett. 314 (1999) 141–151.
[48] P. Auffinger, et al., Molecular dynamics simulations of solvated yeast tRNA(Asp), Biophys. J. 76 (1999) 50–64.
[49] P. Auffinger, E. Westhof, H-bond stability in the tRNA(Asp) anticodon hairpin: 3 ns of multiple molecular dynamics simulations, Biophys. J. 71 (1996) 940–954.
[50] P. Auffinger, E. Westhof, RNA solvation: a molecular dynamics simulation perspective, Biopolymers 56 (2000) 266–274.
[51] P. Auffinger, E. Westhof, Water and ion binding around RNA and DNA (C;G) oligomers, J. Mol. Biol. 300 (2000) 1113–1131.
[52] P. Auffinger, E. Westhof, Melting of the solvent structure around a RNA duplex: a molecular dynamics simulation study, Biophys. Chem. 95 (2002) 203–210.
[53] D.A. Case, et al., AMBER. (7.0 edn), University of California, San Francisco, 2002.
[54] J.R. Horton, et al., Caught in the act: visualization of an intermediate in the DNA base-flipping pathway induced by HhaI methyltransferase, Nucleic Acids Res. 32 (2004) 3877–3886.
[55] N. Huang, A.D. MacKerell Jr., Atomistic view of base flipping in DNA, Philos. Transact. A Math. Phys. Eng. Sci. 362 (2004) 1439–1460.
[56] W. Humphrey, et al., VMD: visual molecular dynamics, J. Mol. Graph. 14 (1996) 33–38 (27–38).
[57] T.E. Cheatham 3rd, et al., A modified version of the Cornell et al. force field with improved sugar pucker phases and helical repeat, J. Biomol. Struct. Dyn. 16 (1999) 845–862.
[58] N.M. Foloppe, AD All-atom empirical force field for nucleic acids. I. Parameter optimization based on small molecule and condensed phase macromolecular target data, J. Comput. Chem. 21 (2000) 86–104.
[59] N.K. Banavali, A.D. MacKerell, All-atom empirical force field for nucleic acids. II. Application to molecular dynamics simulations of DNA and RNA in solution, J. Comput. Chem. 21 (2000) 105–120.
[60] D.R. Langley, Molecular dynamic simulations of environment and sequence dependent DNA conformations: the development of the BMS nucleic acid force field and comparison with experimental results, J. Biomol. Struct. Dyn. 16 (1998) 487–509.
[61] A.D. Mackerell Jr., Empirical force fields for biological macromolecules: overview and issues, J. Comput. Chem. 25 (2004) 1584–1604.
[62] T.E. Cheatham 3rd, Simulation and modeling of nucleic acid structure, dynamics and interactions, Curr. Opin. Struct. Biol. 14 (2004) 360–367.
[63] H. Arthanari, et al., Assessment of the molecular dynamics structure of DNA in solution based on calculated and observed NMR NOESY volumes and dihedral angles from scalar coupling constants, Biopolymers 68 (2003) 3–15.
[64] D.L. Beveridge, K.J. McConnell, Nucleic acids: theory and computer simulation, Y2K, Curr. Opin. Struct. Biol. 10 (2000) 182–196.
[65] P. Auffinger, E. Westhof, RNA solvation: a molecular dynamics simulation perspective, Biopolymers 56 (2001) 266–274.
[66] A. VanderVaart, K.M. Merz, The role of polarization and charge transfer in the solvation of biomolecules, J. Am. Chem. Soc. 121 (1999) 9182–9190.
[67] E. Fadrna, et al., Molecular dynamics simulations of Guanine quadruplex loops: advances and force field limitations, Biophys. J. 87 (2004) 227–242.
[68] S. Shandrick, et al., Monitoring molecular recognition of the ribosomal decoding site, Angew. Chem. Int. Ed. Engl. 43 (2004) 3177–3182.